Temperature-invariant flexible, fatigue resistant and thermal insulating polyimide nanofibrous aerogels with nanofiber-lamella crosslinking architecture

Tiantian Xue[1], Xingyu Zhao[2], Fan Yang[2], Jing Tian[2], Yong Qin[3], Xiaogang Guo[3], Wei Fan[1,2]*, Tianxi Liu[1]

[1] Key Laboratory of Synthetic and Biological Colloids, Ministry of Education, School of Chemical and Material Engineering, Jiangnan University,Wuxi 214122, China

[2] State Key Laboratory for Modification of Chemical Fibers and Polymer Materials, College of Materials Science and Engineering, Donghua University, Shanghai 201620, China

[3] Institute of Advanced Structure Technology, Beijing Institute of Technology, Beijing 100081, China

† Electronic supplementary information (ESI) available. See DOI:

* Corresponding author. E-mail address: weifan@jiangnan.edu.cn or weifan@dhu.edu.cn (Wei Fan)

Experiment

Materials

4,4′-oxidianiline (ODA), pyromellitic dianhydride (PMDA), triethylamine (TEA, 99%) and N, N-dimethylacetamide (DMAc) were commercially purchased from Sinopharm Chemical Reagent Co., Ltd. Deionized (DI) water was used as the solvent throughout the experiments. All chemicals were used as received. Polyrethane (L-1100) was purchased from Shanghai Zaida Plastic Foam Products CO., LTD. Polyurethane was purchased from Changzhou Daye Tengfei Foam Factory. Glass fiber was obtained by Changzhou Zhongrui Fiberglass Products Co., Ltd. Expanded polystyrene (EPS, Compressive strength=600 MPa) and mineral wool (Compressive strength=63 MPa) was obtained by Sichuan Xinchengshun Thermal Insulation Materials Co., Ltd.

Characterization

The morphologies of the nanofibers and aerogels were observed by scanning electron microscope (SEM, HitachiS-8010). In-situ microstructure deformation of PINAs was observed by Gemini SEM300. A 3 nm layer of platinum was coated on the sponges before SEM measurement. Thermogravimetric analysis (TGA) was performed on a NETZSCH TG 209 F1 Libra under air with a heating rate of 10 °C min^{-1} from 100 to 700 °C. The compression test and cyclic compression test were performed on a universal testing machine (SANS, Shenzhen, China) equipped with a 50 N sensor at a compression rate of 40 mm min^{-1}. 10, 000 compression cycles were performed and the curves were recorded. The thermal conductivity of sample (25*25*10 mm) was

measured by a Hot Disk Thermal Constants Analyzer (TPS 2500s) with a kapton sensor (Hot Disk 5465 4.038 mm) according to ISO 22007-2. The applied measurement time and heating power were 10 s and 8 mW, respectively. The apparent density (ρ) of aerogel is calculated by the following equation:

$$\rho = \frac{m}{v} \tag{1}$$

where m is the mass of the aerogel and v is the volume of the aerogel.

The porosity (p) of aerogel is calculated by the following equation:

$$p = 1 - \frac{\rho}{\rho_0} \tag{2}$$

where ρ_0 is the density of the polyimide (ρ_0=1.43 g cm^{-3}).

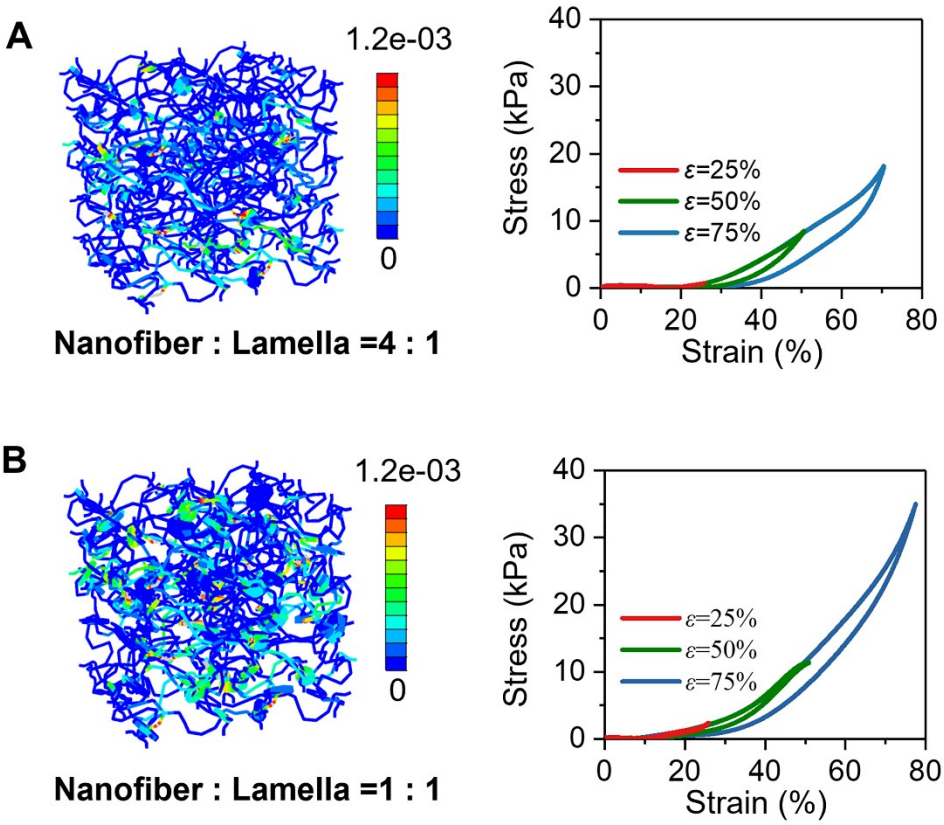

Fig. S1. Stress distribution of nanofibrous aerogel with different ratio under compressive forces simulated by finite element analysis. (A) Nanofiber : Lamella = 4:1. (B) Nanofiber : Lamella = 1:1.

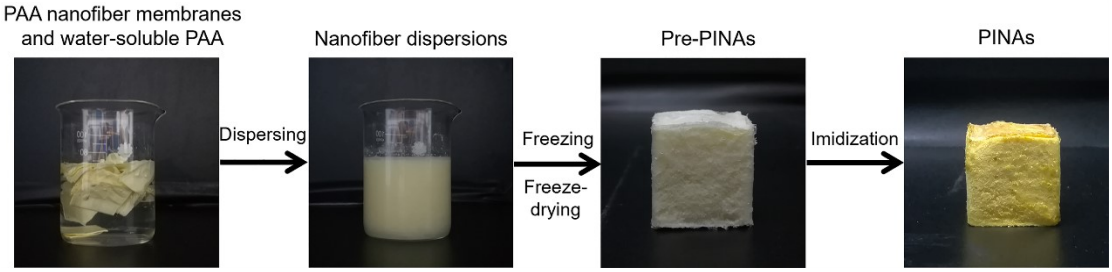

Fig. S2. Photographs showing the fabrication of the PINAs.

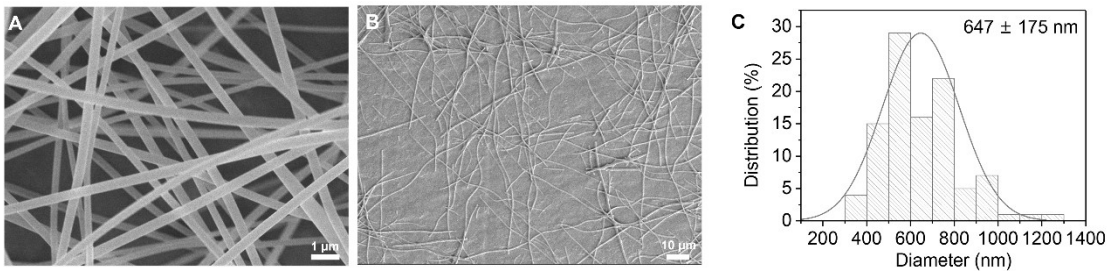

Fig. S3. (A) SEM image of PAA nanofibers. (B) SEM images of homogenized PAA nanofibers. (C) Histogram of diameter distribution of nanofibers.

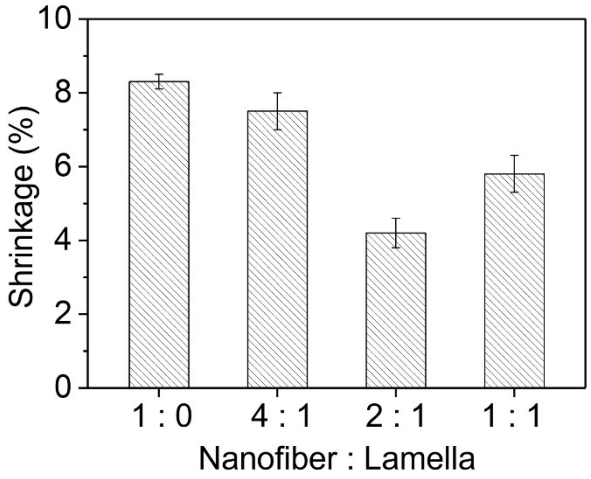

Fig. S4. Shrinkage of PINAs with different nanofiber to lamella ratio.

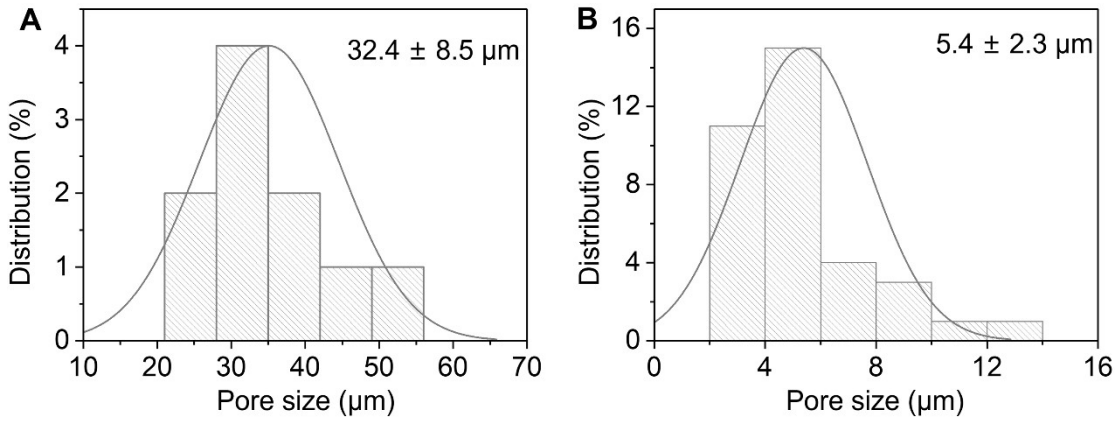

Fig. S5. Histogram of pore size distribution of PINAs. (A) Major pore size. (B) Minor pore size.

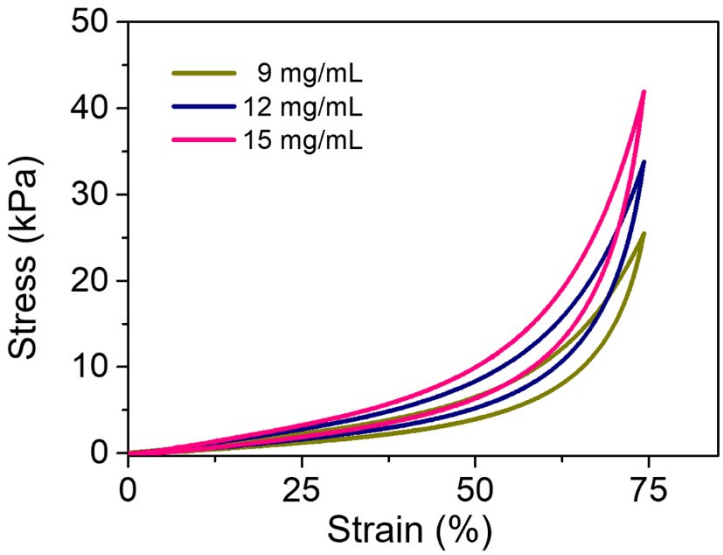

Fig. S6. Elastic resilience of PINAs with different solid content.

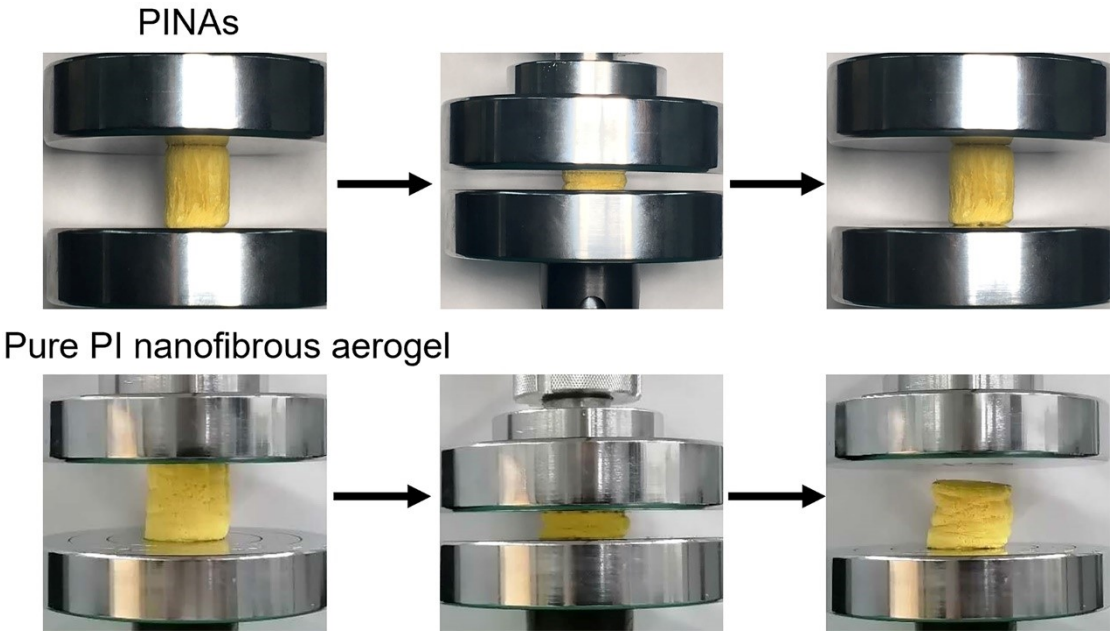

Fig. S7. Elastic resilience of PINAs and pure nanofibrous aerogel.

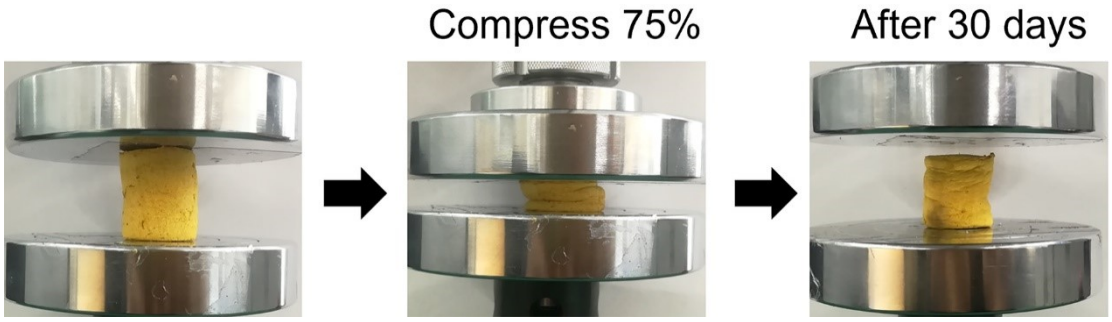

Fig. S8. Fatigue test at 75% strain for 30 days.

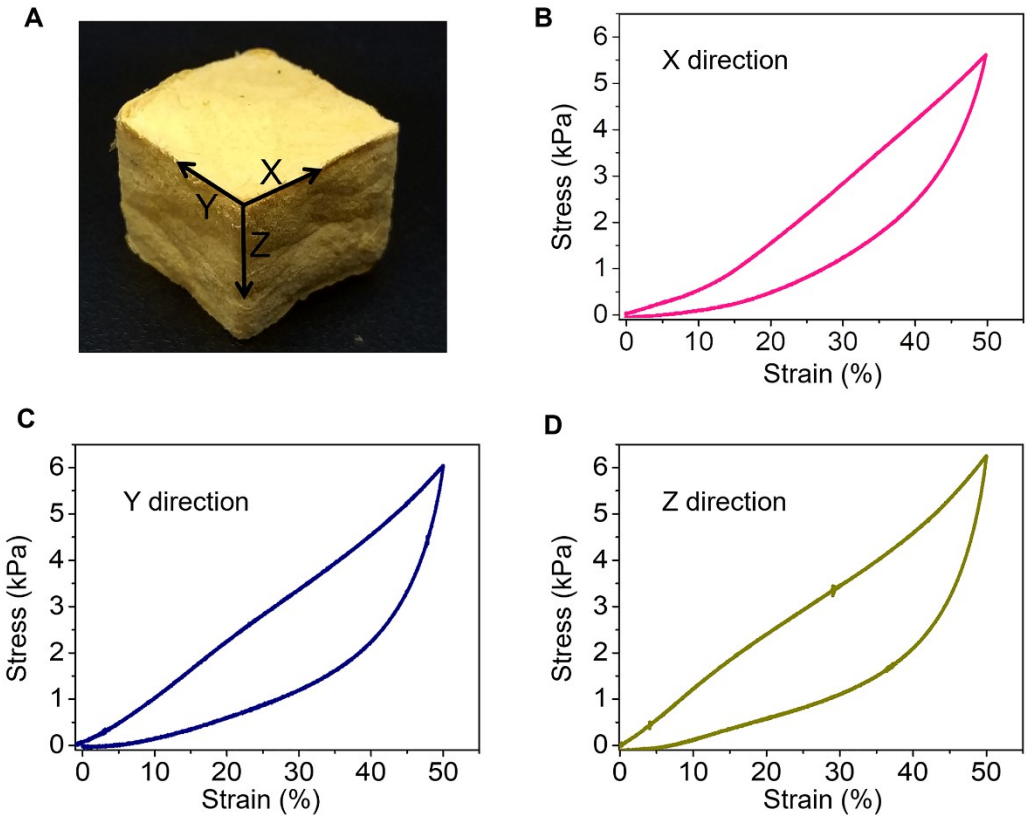

Fig. S9. (A) Photograph of the PINAs. (B-D) Mechanical properties of the PINAs upon different directions.

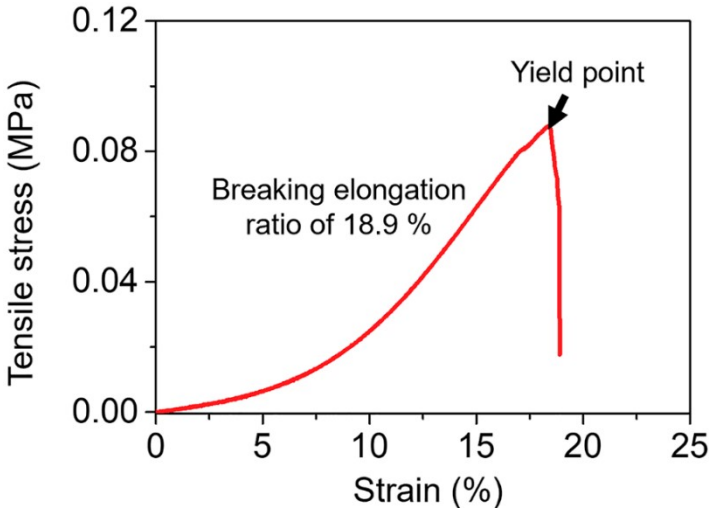

Fig. S10. Tensile stress-strain curve of the PINAs.

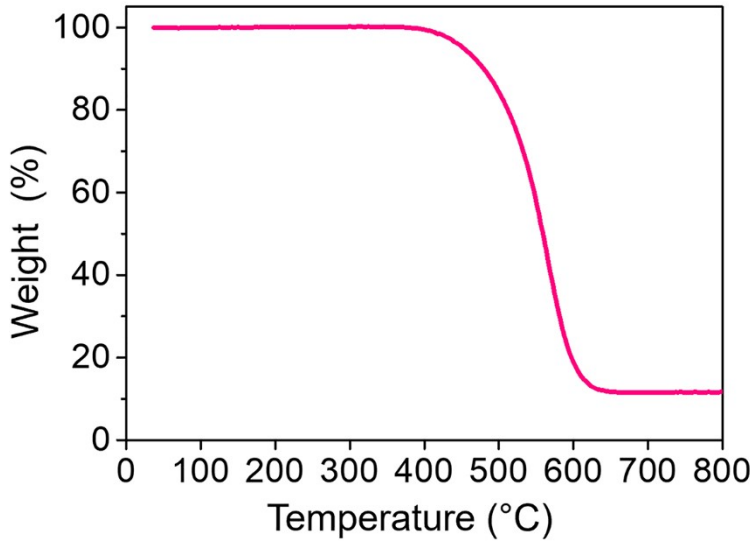

Fig. S11. TGA curves of PINAs (in air).

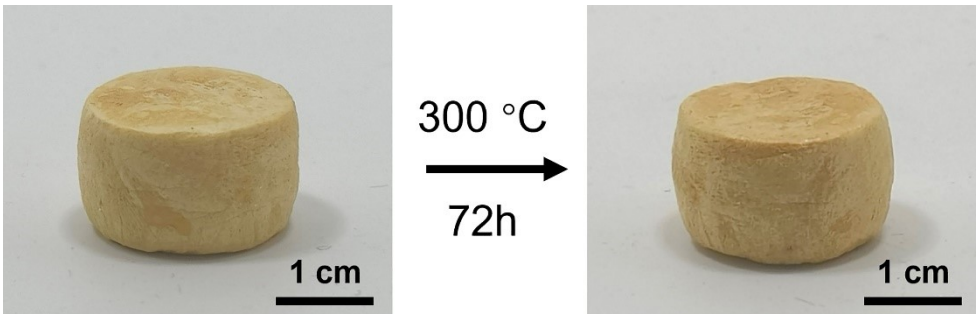

Fig. S12. The images of PINAs before and after heat treatment.

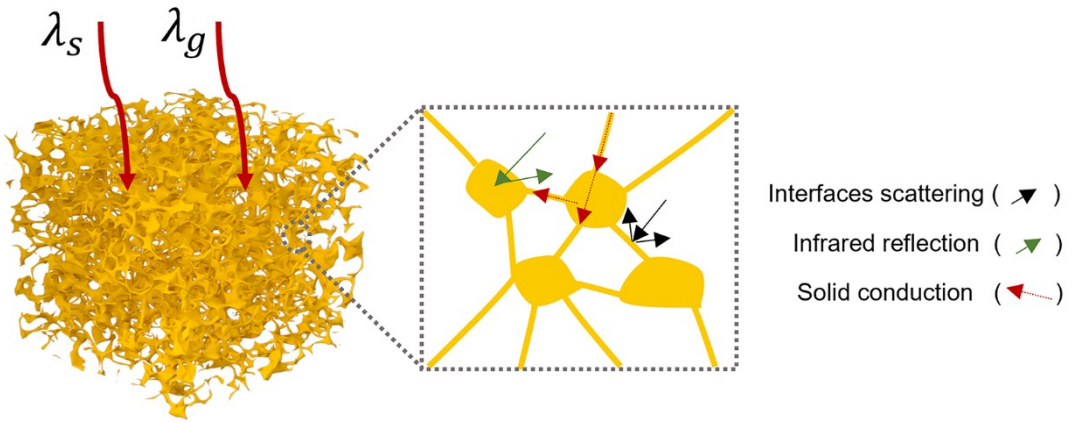

Fig. S13. Mechanisms of thermal conductivity reduction in PINAs.

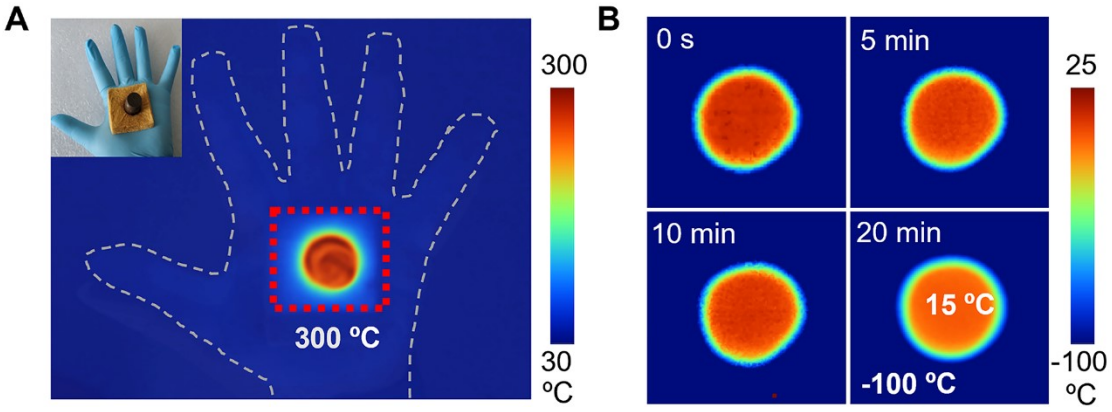

Fig. S14. (A) Thermal insulation ability of PINAs at 300 ºC. (B) Heat preservation ability of PINAs at -100 ºC.

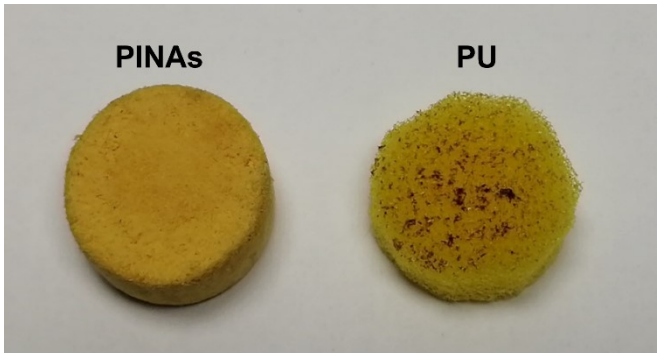

Fig. S15. The bottom of the PINAs and PU foam after placing on the 300 ºC hot stage for 600 s.

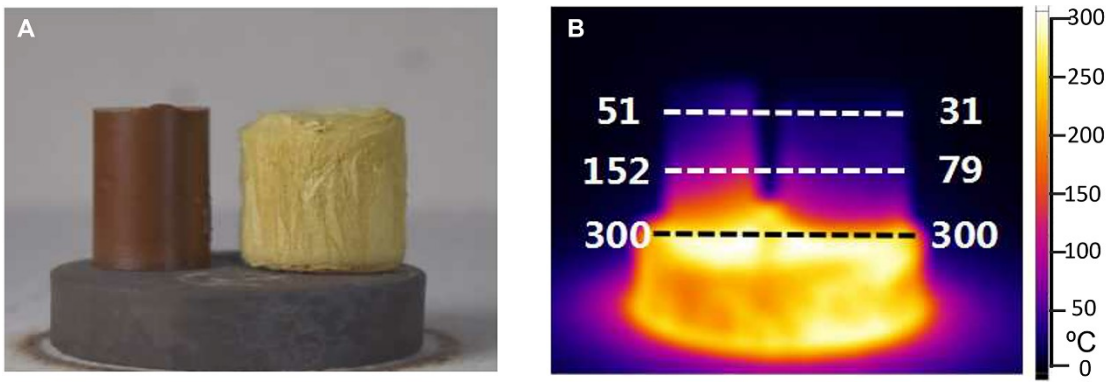

Fig. S16. (A) Photograph of commercial PI and PINAs under 300 ºC stage. (B) Thermal insulation performance of commercial PI and PINAs.

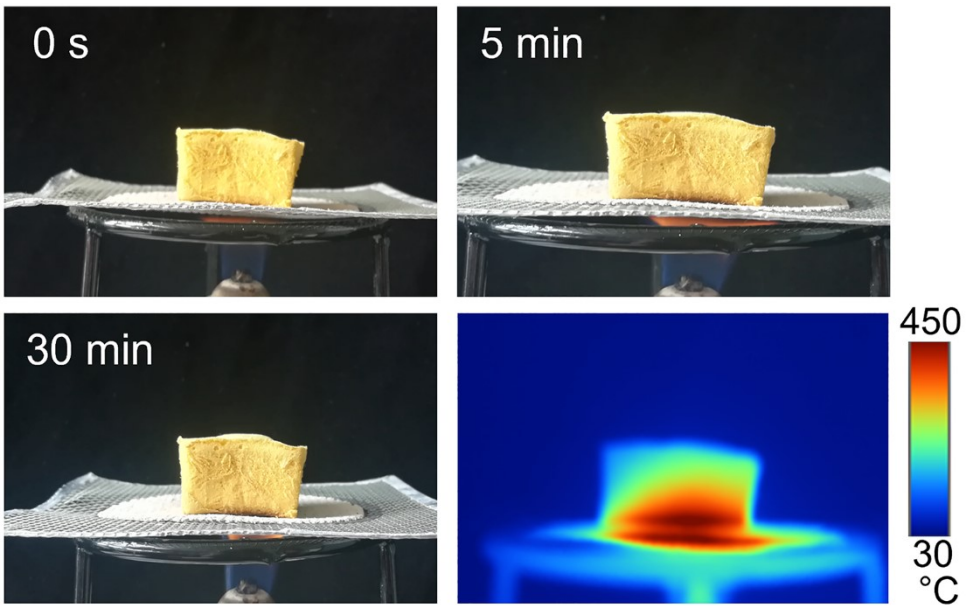

Fig. S17. Optical and infrared images of PINAs on the flame.

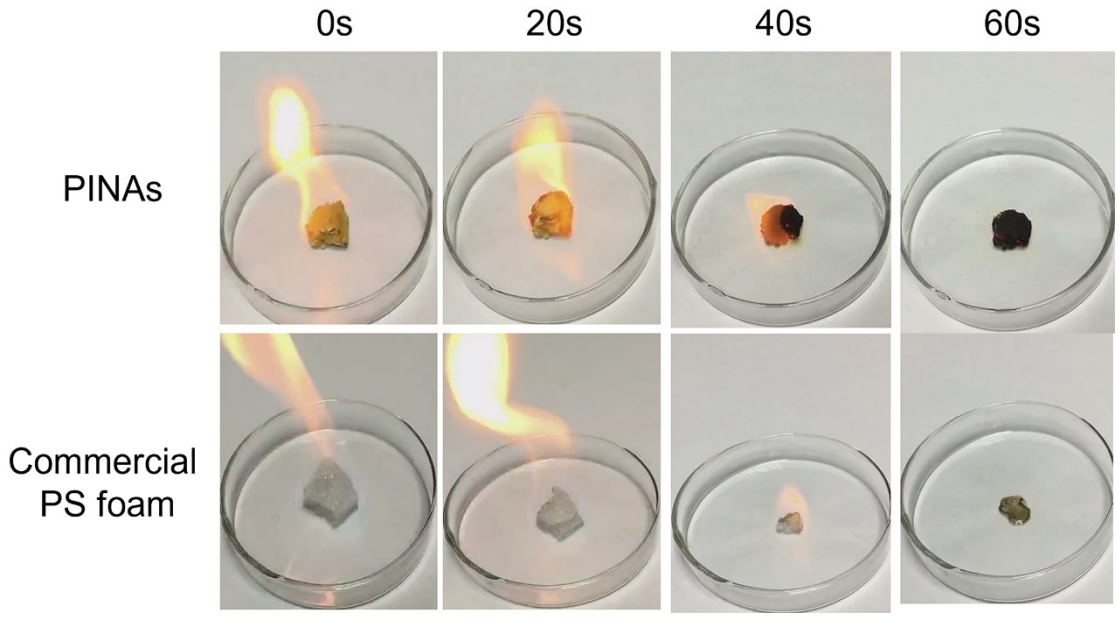

Fig. S18. Burning test of PINAs and commercial PS foam.

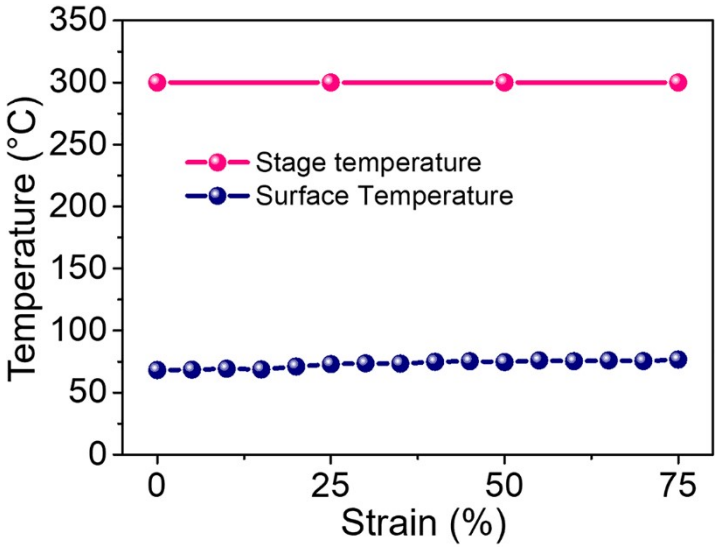

Fig. S19. Surface temperature of the PINAs with different strain on 300 ºC hot stage.